TEST CHAMBER HANDBOOK*

by

Andrew Persily

Ake Blomsterberg

September 1979

Working Paper No. 48

Center for Energy and Environmental Studies
Princeton University
Princeton, N.J. 08544

*Work supported in part by the U.S. Department of Energy Contract No. EC-77-S-02-4288.

Acknowledgments

The authors wish to extend their appreciation to David Harrje and Dr. Frank Sinden for originating and developing the concept of the test chamber. In addition, thanks are extended to Kenneth Gadsby and Roy Crosby for indispensable technical assistance, and to Dr. Jan Beyea for consultation and encouragement in the heat transfer calculations.

Table of Contents

Introduction

During the winter and spring of 1978, a test chamber was designed and constructed at Princeton University for research purposes. The structure is essentially a miniature house, with no internal partitions, built with simplicity and uniformity in mind. Also, the test chamber was built to have minimal infiltration rates, and with versatility to facilitate experimentation. The structure will be used for experiments to attain understandings in the area of energy conservation in housing. Due to the simplicity and controllability of the test chamber, these experiments will reveal phenomena that would be obscured in real homes. Homes in the field have many unknown and uncontrolled variables, and this makes precise studies of small effects difficult. The test chamber is a tool to study subtle effects in the thermal performance of structures.

Physical Description

The test chamber was built to have minimal structural variation and air leakage using methods and materials common in housing. In addition, several features were built-in to enable flexible experimentation.

Basically, the test chamber is a boxlike structure with a square base and dimensions as shown in Figure 1. The structure is supported by a wooden frame of "two-by-fours" and a steel mast, 5.5 m (18 ft) high, running vertically through the center of the structure. The mast extends about 1.5 m (5 ft) above the roof of the test chamber. The test chamber rests on four casters (one in each corner) which enable the entire structure to be rotated about the center mast. Thus, one can control the direction from which the wind or sun impinges on the structure. The casters sit on a wooden platform which in turn rests on the surface of the roof of the Von Neumann Building on the campus of Princeton University.

The general plan of the test chamber is apparent in Figure 1. A detailed sketch of a wall section follows in Figure 2. From inside to outside, the walls are constructed as follows: 2.5 cm of rigid polystyrene insulation; a layer of 6 mil polyethylene; "two-by-four" studs 0.4 m on center, with 8.9 cm of fiberglass insulation between them (since two-by-fours are actually only 8.9 cm thick, the fiberglass fits in with no air space); another layer of the polyethylene; and finally a sheathing of 1.6 cm plywood. This construction ensures low conduction losses, the walls being approximately R-15 according to handbook calculations. The two polyethylene sheets make the walls very air tight.

Two of the outside walls are painted flat black, while the other two are painted with aluminum paint. The roof is of almost identical construction as the walls, except it is painted on the outside with an aluminum roof coating with asbestos. Also, there is a 1.2 m square piece of 1.6 cm plywood on the inside of the roof. The floor of the test chamber is slightly different. From inside to out, there is a flooring of 0.6 cm masonite followed by 2.5 cm of polystyrene, 1.6 cm of plywood, a layer of polyethylene, a layer of "two-by-four" studs and fiberglass insulation, another layer of polyethylene, and finally 0.9 cm of plywood. In both the roof and the floor, the stud spacing is not uniform, as can be seen in Figure 1. There is a door, with a well weatherstripped doorway, in the silver wall without windows. It is a solid wood door, 2.0 m by 0.8 m and 4.4 cm thick. The door is insulated with 7.6 cm of rigid polystyrene so that it has an R-value similar to the rest of the structure. To the left of the door is a small opening for a variety of purposes such as passing out wires. When necessary, this hole is filled with fiberglass insulation and covered with polyethylene.

Flexible experimentation with the test chamber has been made possible by several features. As can be seen in Figure 1, at the base of the steel mast, below the floor of the test chamber, is a hole through which runs an electric cable. One end of the cable is in the test chamber, passing through an additional hole in the mast, while the other end runs down to the Energy Utilization Laboratory in the Von Neumann Building. The purpose of this cable is to transmit data (temperatures, energy use, etc.) from the structure

down to the lab where they are recorded for later analysis. This data system will be described in more detail in the section on instrumentation. The two holes in the mast are also used to run a power cable into the test chamber to provide electricity for equipment within the structure.

A second feature of the test chamber which will enable a wide range of experiments is the existence of four "windows," two each on opposite sides. As can be seen in the photographs in Figure 3, one window is high while the other is low. These windows consist of a wooden frame in the wall into which a variety of panels can be easily installed. In Figure 3, masonite panels, with seven 2.5 cm holes plugged with corks, are in place. The panels are 0.76 m by 0.64 m, and are held tightly in place with metal clamps. (See Figure 4). An air tight fit is insured by the placement of closed cell foam weatherstripping between the window panel and the wooden frame against which it is held. The panels will enable one to study, for example, the effects of different sizes, shapes and arrangements of openings on the air infiltration rate of the structure. When no openings are desired, panels of fiberglass insulation and masonite, with an R-value similar to the walls, are fitted into the windows. The experimental opportunities made possible by the interchangeable panels are great. As would be expected from this physical description, the test chamber is indeed very air tight, uniform in terms of heat conduction through the shell and also adaptable to a wide range of experiments.

Heat Losses of the Test Chamber

The heat losses (and in some cases gains) of the test chamber consist of conduction, air infiltration, and radiation to and from the environment. The calculations of these heat losses are presented below, except for radiation which will be discussed at length in a future paper. The results of these calculations are examined, and an overall lossiness is presented in units of watts of internal power necessary for each degree Celsius of temperature difference between indoors and out.

The major portion of heat loss from the test chamber is conduction of heat through the shell. As shown below, the walls and roof have R-values of about 15 in English units, while the floor has a somewhat higher thermal resistance. By assuming predominantly one-dimensional heat flow and by estimating losses at the corners and edges, one obtains a value of the lossiness due to conduction through the shell of about 16W/°C.

A second source of conduction heat losses, in addition to that through the walls, is the steel mast running through the center of the structure. In order to minimize the mast's contribution to the heat losses, an attempt was made to isolate the mast from the inside of the test chamber. This was done by wrapping the mast with batts of fiberglass insulation to minimize conduction, and then by covering the insulation with aluminum foil to cut down radiative heat transfer to the mast. In addition, the mast was filled with vermiculite in order to eliminate any convective heat transfer within the pipe. As shown below, after making some reasonable assumptions, the losses due to the pipe are estimated to be about 0.5 W/°C at the most. This upper limit is only 3% of the conduction through the shell.

Another source of heat loss is the infiltration of outside air into the test chamber. The structure was built to have very low infiltration rates, and the measured rates are indeed very small. It will be shown that for each tenth of a "house volume" exchanged in one hour there is a net loss of 0.5 W/°C. Since the measured rates are on the order of 0.1 exchanges per hour or less, infiltration losses are small compared to conduction losses.

Radiative heat gains and losses of the test chamber present a very complex problem. Daytime solar gains are dependent on cloud cover and other factors, and the actual heat added to the interior of the structure is a complicated, time dependent problem. The radiative heat loss at night depends on the amount of long wave radiation from the sky and the surroundings. Experiments studying the nighttime radiation heat loss have been conducted and will be discussed in a future paper.

Presented below are the calculations of the conduction losses through the shell, and the losses due to the steel mast and air infiltration.

Conduction Through the Shell

The conduction of heat through the test chamber shell dominates its heat exchange with the environment. Conduction losses are determined by the building materials, and their arrangement and thicknesses. The calculations presented here are based on similar calculations in Appendix A of Saving Energy in the Home.[1]

Table 1 lists the materials used in the test chamber, along with several important physical and thermal properties including: density, ρ; heat capacity per unit mass, c; thermal conductivity, k; and material thickness in the direction of heat flow, d. From these values, the conductance, U,

and the capacitance, heat capacity per unit area, C_s, are calculated and also listed in Table 1. The numerical values were obtained from Saving Energy in the Home[1] and the 1977 ASHRAE Handbook of Fundamentals.[2]

With the conductances and capacitances of Table 1, the U-values and capacitances of the walls, roof and floor can be calculated according to the following expressions:

$$U = \left[\sum_{i=1}^{N}(1/U_i)\right]^{-1} = \left[\sum_{i=1}^{N}R_i\right]^{-1}$$

$$C = \sum_{i=1}^{N}C_{si}$$

N is the number of layers in the surface. U_i and C_{si} are the conductance and capacitance of the ith layer. And $R_i = (U_i)^{-1}$ is the thermal resistance of the ith layer. The calculations of U and C for the walls, roof and floor are shown in Table 2.

A comment on Table 2 is necessary concerning the stud/insulation layers. These layers were handled identically to the manner in Saving Energy in the Home. The heat transfer is assumed one-dimensional, which is quite reasonable in this case where the thickness of the studs and insulation are the same. Average values of U and C_s are determined by weighting the two components by the areas they occupy. For the walls with studs 0.4 m on center, the result is U = 0.605 W/m^2-°C and C_s = 1.9 Wh/m^2-°C. The stud spacing in the floor and roof is not uniform, but an average value of 0.3 m is used, resulting in U = 0.624 W/m^2-°C and C_s = 2.4 Wh/m^2-°C. The thermal resistance and capacitance of the polyethylene sheets are so small that they are neglected. Also, in the roof calculation, the 1.2 m square piece of plywood on the inside is

approximated as a thinner sheet of plywood which covers the entire ceiling. The door and window panels with insulation in place both have R-values somewhat larger than the walls, but due to the small area they occupy, the correction to the wall U-value results in less than a 1% effect on the overall heat loss. Therefore, these differences are ignored.

In most calculations of conduction losses, the structure considered is of larger proportions than this test chamber. It is common practice in determining such losses for a home to simply multiply the area of a wall (ceiling, etc.) by its U-value and then add the contributions of each area, neglecting the effects of the corners and edges where the heat flow is no longer one-dimensional. The results of such a calculation for the test chamber is presented in Table 3, and gives a first order lossiness of 15.2 W/°C. In homes, the wall area is so large compared to its thickness, that corner effects are negligible and this first order lossiness is adequate. But in determining the conduction losses of the test chamber, an unusual situation is encountered in which the wall area is small. It is not clear whether corner effects can be ignored, and this question has to be answered.

If the walls were of homogeneous construction, the heat losses at the corners and edges could have been easily calculated through the use of shape factors.[3] But the walls are constructed of several layers. If these layers continued uniformly to the edges where the walls meet, the calculations would have been more complex, but still manageable. Unfortunately, the edges are not of this construction. Instead, at the edges, the 8.9 cm stud/insulation layer is almost all stud. A cross section of the corner is shown in Figure 5A. The effective "post" of wood in the corner is a source of complication in the calculations. The approach taken is to calculate upper and lower limits for the corner effects.

The corner calculations are done considering a wall section 1 m high and extending from the center of the wall to the corner. (See Figure 5B). The lower limit of the lossiness of this section is obtained by considering the corner to be a perfect insulator. Thus we need consider only one-dimensional heat flow through a wall section with a width equal to one-half the inside width of the test chamber, 1/2 (2.18 m) = 1.09 m. The area of this section is thus 1.09 m^2, which, when multiplied by the wall's U-value of 0.38 W/m^2-°C, yields a low value for the heat loss constant of 0.41 W/°C.

The upper limit is obtained by a more complex method based on an article by I. Langmuir, et al.[4] The details of this calculation are presented in Appendix A. This method yields an upper limit by doing the calculations as if a series of infinitely thin, but perfectly conducting, sheets are embedded in the wall, parallel to the wall itself. Thus, the isotherms are all parallel to, and the heat flow is perpendicular to, the wall. The calculations are done by considering infinitesimally thin wall sections through all of which the same amount of heat must pass. These differential elements are added together for each layer of material, and thus five equations (one for each layer: two air layers, plywood, stud/insulation, and polystyrene) of the form $Q = H_i \times \Delta T_i$ are obtained. H_i and ΔT_i are the heat loss constant and temperature difference, respectively, of each layer. Since the Q passing through each layer must be the same, these equations can be solved to obtain an equation of the form, $Q = H_{net} (T_{in} - T_{out})$. H_{net} is the desired upper limit and has a value of 0.44 W/°C as presented in Appendix A. Multiplying the upper and lower limits by the inside wall height, 3.53 m, one obtains 1.55 W/°C and 1.45 W/°C upper and lower limits of the heat loss of half of a wall. There is only a 7% difference be-

tween these two numbers. Further consideration leads to choosing a value of 1.50 W/°C as the heat loss of a half wall section.

Multiplying 1.50 W/°C by the eight half wall sections, one obtains 12.0 W/°C as the heat loss for the walls. One must add to this 1.8 W°C for the roof and 1.7 W/°C for the floor as in the first order lossiness calculation. In addition, there are the eight edges where the four walls meet the roof and floor. Ths inside length of the edges is 2.18 m, and therefore the shape factor for all eight of them is S = 8 x .54 x 2.18 m = 9.42 m. Using a value of the thermal conductivity for the edges of k = 0.048 W/m-°C, one obtains a heat loss constant for the edges of kS = 0.5 W/°C. Adding all these contributions together, the net lossiness due to conduction alone is L_c = 12.0 + 1.8 + 1.7 + 0.5 = 16.0 W/°C. This value is 5% larger than the first order lossiness of 15.2 W/°C. In addition to conduction of heat through the shell, air infiltration and conduction of the steel pipe must also be considered.

Air Infiltration

The test chamber was constructed to be very tight with respect to air leakage, but there is still some heat loss due to air infiltration. Air infiltration rates are dependent on the outside weather and are therefore variable, but measurements show that the structure has air infiltration rates on the order of 0.1 exchanges/hour. If one assumes the heat loss rate associated with air infiltration is equal to $\rho c_p \cdot AI \cdot \Delta T$, then this heat loss can be easily calculated. The lossiness due to air infiltration is therefore $L_{AI} = \rho c_p$ AI. Assuming an air infiltration rate of

one-tenth of an interior volume per hour, AI = V/10·hr. V, the volume of the test chamber is 16.6 m^3. ρc_p of air in the range of room temperature is 0.33 Wh/m^3-°C. Thus, L_{AI} = 0.5 W/°C. This number will vary with the outside weather, but since it is only a 3% correction to L_c = 16.0 W/°C, this variation may be neglected.

Losses Through the Steel Mast

The steel mast running through the center of the test chamber gives it extra support and enables the structure to be rotated. But it also presents a complex heat transfer problem. As mentioned earlier, the mast was partially isolated from the interior of the test chamber. Conduction from the test chamber interior to the mast is reduced by wrapping the mast with batts of fiberglass insulation. The insulation is somewhat compressed in wrapping the mast, and this compression decreases the insulating properties of the fiberglass. The fiberglass was then wrapped in aluminum foil to cut down on long wave radiation from the heaters. Since the mast is hollow, it was filled with vermiculite to eliminate any convective heat flow inside of it. Using several simplifying assumptions, an estimate of the heat conducted through the mast to the outdoors is made in Appendix B. This estimate is about 0.5 W/°C, only 3% of the 16.0 W/°C due to conduction through the shell.

Combining the computed heat losses due to conduction through the shell and the steel mast, and air infiltration, a net lossiness of 17.0 W/°C is obtained. There is some uncertainty in this value due to construction

imperfections. Also, air infiltration rates different from the assumed 0.1 exchanges/hour will cause a small amount of variation in the lossiness. The only significant factor which has been left out is radiative exchange with the external environment, a strong function of outside conditions. The question of radiation will be studied and discussed in a future paper.

Instrumentation

The test chamber is instrumented with a variety of devices to measure and record several variables, and also to affect conditions within the structure. The structure is heated with several electric light bulbs strung vertically, usually 60 or 100 watt bulbs. This "heater" is controlled by either a common Honeywell thermostat (model T87F), or by a simple on/off switch running outside the test chamber. A small electric fan is used at times to mix the interior air in order to prevent significant temperature stratification.

Indoor and outdoor temperatures are measured with YSI precision thermistors. The air temperature probe No. 705 with the 44018 thermistor composite is used. Instantaneous wind speed and direction are measured about 1.5 m above the test chamber. Also, these same variables plus the average wind speed are measured at the other end of the roof of the Von Neumann Building, about 5.5 m above the roof surface. The energy consumed within the test chamber by the heaters and other equipment is measured with a General Electric wattmeter similar to those used in homes. The wattmeter is equipped with a photo-interrupter module which counts the revolutions of the disk in the meter. All of these variables measured in or near the test chamber are transmitted by electric cable down to the lab in the Von Neumann Building. The cable is connected to an Esterline Angus Programmable Data Acquisition System (PDAS), Model CD 2020. The PDAS is basically a multiplexing device which reads up to twenty voltages at controllable time intervals. The output of the PDAS goes into a teletype which records the data on paper. Also, the output can be recorded onto magnetic data cassettes which can then be read directly into a computer for analysis. There is much room for additional measurements on

the PDAS, such as pressure across walls, solar radiation, etc.

For air infiltration measurements, an automated air infiltration unit (AAIU) is installed in the test chamber. The AAIU [5-7] measures the decay in concentration of a tracer gas (SF_6) in the test chamber, and records these concentrations on a data cassette. The AAIU is equipped with an automatic injection system built for use in homes, but this system injects amounts of SF_6 too large for the small test chamber. Instead, SF_6 is injected by hand with a syringe, a few cc's at a time. Since the test chamber is so tight, one such injection will last around ten hours before the concentration gets too low for accurate measurements. The electric fan is used to mix the SF_6 uniformly throughout the interior of the test chamber.

The present instrumentation set up has proved to be convenient and flexible and no significant changes are planned. The opportunity always exists for measuring new variables and feeding these into the PDAS.

Experimentation

Preliminary experiments have been conducted in the test chamber to study its physical performance. These experiments have measured the temperature stratification within the structure, its heat loss rate, and its overall time constant. Also, measurements of the air infiltration rate of the test chamber have been made. These experiments will be discussed presently, followed by the experiments intended for the future.

Completed Experiments

The first experiments conducted were measurements of temperature gradients within the structure. These were done in order to justify the use of a single indoor temperature. The tests were conducted with and without the heater running, and with and without the small electric fan mixing the air. Two thermistors were used, one placed about 40 cm from the floor while the other was placed the same distance from the ceiling. It was found that without the fan running and with the heat on, a temperature difference between the two thermistors of about 1.7 °C existed. The use of the fan reduced the difference to at most 1.0 °C with the heat running, and 0.4 °C with the heat off. In all cases, the warmer air was at the top of the test chamber. This leads one to consider possible reductions in this temperature difference by placing more of the light bulb heaters near the bottom of the test chamber. Regardless, a single interior temperature may presently be used with an uncertainty of $\pm$ 0.5 °C. In addition, an experiment was conducted to check for a lateral gradient between the side with the heaters and the side without, but no

significant temperature difference was found.

Once an internal temperature gradient was shown not to be of great concern, experiments were conducted to begin checking the measured lossiness against the computed lossiness of 17.0 W/°C. Typically, the thermostat was set and the test chamber was closed tightly. The tests were conducted at night in order to avoid considering the heat gain due to solar radiation. Overnight, the heaters cycled, while the inside and outside temperatures, and the energy consumption were being recorded. Although the nighttime tests lasted up to twelve hours, the first and last few hours were neglected in the determination of the lossiness. During the first few hours, transient effects of daytime temperatures and solar radiation were allowed to die out. And the last few hours were not considered because of the morning temperature increase. Thus, a typical period of consideration was from midnight to six in the morning.

The experimental lossiness of the structure was computed as follows. The integrated energy consumption, E, during the length of the test period, t, is obtained from the Esterline Angus PDAS. Using the recorded temperatures, the average temperature difference during the test, $\overline{\Delta T}$, is computed. The lossiness L, defined as the power (Watts) required to maintain a unit temperature difference (°C) between inside and out, is given by $L = E / \overline{\Delta T} \times t$. Five separate measurements of the lossiness were made, and a range of values was obtained. The measured values were 17.9, 18.5, 16.2, 14.9 and 20.0 W/°C. This is roughly a 15% spread on either side of the computed lossiness of 17.0 W/°C. This large degree of variation cannot be accounted for by differing

air infiltration rates, because these rates are too low to make such a large difference. This wide variation is curious and the reasons for it are unclear at this time. One possible explanation is differing amounts of radiative heat transfer with the sky and surroundings on different nights. Additional experiments are planned in which this radiation will be measured.

Preliminary experiments were also conducted to measure an overall time constant for the test chamber. In one series of tests, the heater was turned on for about two hours to establish a large temperature difference between inside and out. The heaters were then turned off from outside the test chamber, and the inside temperature was allowed to decay. The actual decay history was compared with calculations based on a model of the structure as a single heat capacity with heat loss proportional to the inside/outside temperature difference.[8] The integral solution for the inside temperature for this model is,

$$T(t) = e^{-t/\tau} \{ T_o + [\int_o^t e^{t'/\tau} [Q(t')/L + T_{out}(t')] dt']/\tau \}$$

where t is time, T_o the initial inside temperature, Q(t) the sum of all energy inputs, L the lossiness, $T_{out}(t)$ the outside temperature, and τ the time constant equal to MC/L. M is the structure's mass and C is the average heat capacity. By fitting the measured inside temperature to the above equation, τ and L are found in pairs. For a given L, the corresponding τ is that which minimizes the sum of the squares of the differences between the measured inside temperature and that temperature predicted by the integral equation. One thus obtains a series of τ and L pairs, each with a minimum sum of squared errors.

In Figure 6 one finds the results of such a test. The horizontal axis is the time constant τ in minutes, while the vertical axis is the sum of the squared differences between the measured and predicted inside temperatures. This particular test had 140 time steps of five minutes each. In the figure there are six concave upward curves; each curve corresponds to a different assumed value of lossiness, L, as indicated. For the computed value of $L = 17.0$ W/°C, which certainly is in the range of measured values, the best fitting time constant is about $\tau = 200$ minutes. But if one uses lower values of the lossiness, the fit improves significantly. The best fit is for τ between 80 and 120 minutes and a lossiness somewhat less than 10 W/°C, which is definitely smaller than the actual lossiness of the structure. These results occurred when the heat was off and the inside temperature decreased.

In another test the heat was on, and the structure warmed up. When the appropriate integral solution was fitted, a similar time constant on the order of 80 to 100 minutes was found. But along with this best fitting time constant went a lossiness on the order of 28 W/°C. This seemingly strange result of very high and low lossinesses providing the best fit occurs because the simple model used is not appropriate. A more complex model and further study is necessary if this effect is to be understood properly.

A series of tests were conducted to measure the air infiltration rates of the test chamber. This was done using the Automated Air Infiltration Unit mentioned in the section on instrumentation. The results of these tests are plotted in Figure 7. The air infiltration rates in units of volumes exchanged per hour is plotted against the hourly average wind speed. There is considerable

scatter due to a variety of temperature differences between inside and out. Even with very strong winds and temperature differences as high as 44°C, the air infiltration rates are only on the order of one or two tenths per hour. Only during the coldest and windiest hours does the exchange rate get up near 0.2 X/hr. Typically, the air infiltration rate is on the order of only 0.1 X/hr. These are very low infiltration rates, and it may be possible to lower them further through additional tightening. But the goal of building a very tight structure has indeed been accomplished.

Future Experiments

The test chamber was built and designed predominantly with research into air infiltration in mind. The shell was made very tight in order to avoid the problem of unknown leakage sites that complicates such research in homes. In homes in the field, we never know where the leaks are. But in the test chamber, when we put an opening in a window panel, we can be certain that this is the only significant leak. Therefore, the test chamber provides an excellent opportunity for research into air infiltration.

The first planned air infiltration tests will examine the interaction of wind, temperature differences, and the position of openings in causing air infiltration. This interaction has never been completely documented. Sinden has discussed this interaction theoretically,[9] and has predicted several relations. Experiments in the test chamber will enable us to examine those relationships.

The mechanisms by which air enters or leaves openings in a structure is another area to be studied in the test chamber. Attention will be focused

particularly on unsteady mechanisms of air infiltration such as pulsating flows through one or more openings, and penetration of eddies.[10] The studies will focus on these turbulent effects, rather than averaging them out by using an hourly mean wind speed. These experiments will provide knowledge of the nature of the flow in and out of openings in the shell, and of the extent of pulsating as opposed to steady flow through the openings. Knowledge of the extent of pulsation and the general characteristics of the flow may prove useful in the design of heat recovery devices. Such devices may be able to achieve healthy levels of ventilation while reducing the amount of energy necessary to heat up the incoming air. A significant amount of pulsation may make it possible to use passive heat recovery devices instead of powered ones.

As mentioned earlier, additional measurements of the lossiness of the test chamber are planned in order to understand the variation in the previous measurements. The new tests will include detailed considerations of the long-wave radiative interchange between the structure and its environment. Also, additional experiments and calculations will be necessary to explain the time constant experiments discussed earlier. A model explaining the time dependent transmission of heat through the shell is needed. The theory of transmission matrices and other methods employed by Robert Sonderegger could be used.[11]

Appendix A Upper Limit on Corner Losses

The upper limit of corner losses is made by assuming that a series of infinitely thin, perfectly conducting sheets are embedded parallel to the wall. The isotherms are therefore also parallel to the wall, and the heat flows perpendicularly to the wall. The wall section considered is shown in Figure A1. It extends from the middle of the wall to the corner, and it is 1 m high. As shown in the figure, the wall is divided into several sections. Each section is considered separately, but as a result of the assumptions made, the border between each section is an isotherm and the heat flow through each section is the same.

The first layer is the inside air film with an area of $A_i = 1.09\ m^2$ and a heat transfer coefficient of $h_i = 8.28\ W/m^2\text{-}^\circ C$. This layer separates the test chamber interior at a temperature T_i from the inner surface of the wall at T_1. Thus the heat flow across this air layer is $Q = h_i A_i (T_i - T_1)$. The next layer in the wall is the 2.5 cm of polystyrene insulation. As in Figure A1, this layer separates temperature T_1 from T_2. Polystyrene has a thermal conductivity of $k_1 = 0.035\ W/m\text{-}^\circ C$. Therefore, the heat flowing across the polystyrene is given by $Q = k_1 S_1 (T_1 - T_2)$ where S_1 is the shape factor[3] for this layer. The shape factor for this layer is equal to its width of 1.09 m divided by its thickness 0.025 m plus .27 for the corner, all multiplied by its 1 m length. Thus, $S_1 = (1.09m/0.025m + .27) \cdot 1m = 43.9\ m$.

The most complex layer in the wall is that of the studs and insulation, shown in Figure A2. The dimensions are $x_o = 1.12$ m and $y_o = 0.089$ m, and it consists of two parts labeled α and β. The α section of studs and insulation is treated as a uniform material with a thermal conductivity obtained from that of the studs and insulation by weighting their areas. That is, $k_\alpha = (.906)(0.047\ W/m\text{-}^\circ C) + (.094)(0.118\ W/m\text{-}^\circ C) = 0.054\ W/m\text{-}^\circ C$. The β section is assumed

to be all stud, which is on the safe side since this is a high estimate anyway. k_β = 0.118 W/m-°C. The approach taken is to consider an elemental section of thickness dy which is a distance y from the inside of the layer. The area of such an elemental section is $(x_o + y) \cdot 1m$, and the temperature difference across the section is dT. Remembering that the temperature is uniform across the layer for any given value of y, the heat flow across any such elemental section consists of two parts and is equal to:

$$Q = k_\alpha/dy\ (x_o \cdot 1m)\ dT + k\beta/dy\ (y \cdot 1m)\ dT$$

$$= (k_\alpha x_o + k_{\beta y}) \cdot 1m \cdot dT/dy.$$

The temperature difference across the entire layer is $T_2 - T_3 = \Delta T = \int_{y=0}^{y=y_o} dT$. Thus,

$$\Delta T/Q = 1/Q \int_{y=0}^{y=y_o} dT = \int_0^{y_o} [dy\ /\ (x_o k_\alpha + y k_\beta)\ (1m)]$$

$$= [1/k_\beta(1m)]\ \ln\ (1 + y_o k_\alpha / x_o k_\beta)$$

or,

$$Q = k_\beta [\ln\ (1 + y_o k_\beta / x_o k_\alpha)]^{-1}\ (1m)\ \Delta T$$

$$= 0.737\ W/°C\ (T_2 - T_3).$$

The next layer is the outer sheathing of plywood which is treated just like the polystyrene layer. The plywood separates T_3 and T_4, and has a thermal conductivity of k_3 = 0.115 W/m-°C. Its shape factor is equal to S_3 = (1.20m/ 0.016m + .27)·1m = 75.3 m. Finally, there is the outside film coefficient which equals h_o = 26.2 W/m^2-°C and acts over an area of A_o = 1.23 m^2. This

outside air layer separates T_4 from T_o as in Figure A1.

Thus, for the five separate layers, there are the five following expressions for the heat flow through the wall Q:

Inside Air	$Q = h_i A_i (T_i - T_1)$	$= 9.03$ W/°C $(T_i - T_1)$
Polystyrene	$Q = k_1 S_1 (T_1 - T_2)$	$= 1.54$ W/°C $(T_1 - T_2)$
Studs/Insulation	Q	$= 0.737$ W/°C $(T_2 - T_3)$
Plywood	$Q = k_3 S_3 (T_3 - T_4)$	$= 8.66$ W/°C $(T_3 - T_4)$
Outside Air	$Q = h_o A_o (T_4 - T_o)$	$= 32.2$ W/°C $(T_4 - T_o)$

From these five expressions, we can obtain the desired expression for Q in terms of only T_i and T_o, i.e. $Q = H_{net} (T_i - T_o)$. The result of this algebraic calculation is $H_{net} = 0.442$ W/°C.

Appendix B Estimate of Losses Through the Mast

In this calculation the section of mast within the test chamber is considered as three sections, each at a single temperature T_1, T_2, and T_3. Thermal resistances between the sections are estimated, along with the resistances between these sections and the interior temperature T_i. A sketch of the network is shown in Figure B1. R_1 is the resistance between one-third of the pipe insulation and the interior. R_3 is the resistance between the pipe sections themselves. There are two resistances to the outside temperature T_o, one out the top, R_2 and one through the bottom, R_2. Once these resistances have been determined, one can compute an overall resistance between T_i and T_o.

The important physical parameters of the mast and its insulation are as follows. The inner radius of the mast is $r_1 = 0.051$ m, and the outer radius is $r_2 = 0.057$ m. The radius of the layer of insulation if $r_3 = 0.14$ m. The steel has a thermal conductivity of $k_1 = 52$ W/m-°C, while the compressed fiberglass insulation has an estimated thermal conductivity of $k_2 = 0.066$ W/m-°C.

The thermal resistance, R_1, between the pipe and the test chamber interior consists of the sum of the resistances of the fiberglass insulation and the inside film layer. This sum takes the form $R_1 = \ln (r_3/r_2)/2\pi k_2 L + 1/2\pi r_3 hL$, where L is one-third of the inside length of the mast, $L = 1/3\ (3.53\ m) = 1.18$ m, and h is the inside film coefficient, $h = 8.28$ W/m^2-°C. Thus,

$$R_1 = 1.84\ °C/W + 0.12\ °C/W = 1.96\ °C/W.$$

The thermal resistance R_3 is the resistance of one-third the inside length of the mast in the direction parallel to the mast. Since the thermal

conductivity of the steel is so much larger than that of the vermiculite or fiberglass, one may safely assume that this resistance is only due to the steel acting through an area of $A = \pi r_2^2 - \pi r_1^2 = 2.0 \times 10^{-3}\ m^2$. Thus, $R_3 = (1.18\ m)/(2 \times 10^{-3}\ m^2)\ (52\ W/m\text{-}°C) = 11.3\ °C/W$.

Finally, there are the resistance between T_1 and the outside temperature, R_2. and between T_3 and T_o, R_2'. In order to simplify these calculations. I assume that once the mast reaches the outside through the roof or floor, the steel immediately reaches the outside temperature. This will cause the estimate to be on the high side. Since the pipe is surrounded by fiberglass insulation as it passes through the roof and floor, these resistances are calculated as R_3 was, except the length of pipe considered is the thickness of the roof and floor. These thicknesses are 0.14 m and 0.30 m respectively. Thus,

$$R_2 = (0.14\ m)/(2 \times 10^{-3}\ m^2)\ (52\ W/m\text{-}°C) = 1.35\ °C/W, \text{ and}$$

$$R_2' = (0.30\ m)/(2 \times 10\text{-}3\ m^2)\ (52\ W/m\text{-}°C) = 2.88\ °C/W.$$

With the required resistances at hand, I calculated the lossiness due to conduction through the pipe. I did this calculation numerically by setting $T_i = 20°C$ and $T_o = 10°C$, requiring the heat flows at each node to add to zero, and then solving for the temperatures T_1 and T_3. I then calculated the heat flows out of the top and bottom. The sum of these two heat flows divided by the 10°C temperature difference is the desired lossiness. The result is a lossiness due to the steel mast of 0.54 W/°C.

References

1. Socolow, R. H., ed., Saving Energy in the Home, Princeton's Experiments at Twin Rivers, Ballinger Publishing Company, 1978.

2. ASHRAE Handbook of Fundamentals, American Society of Heating, Refrigerating and Air-Conditioning Engineers, Inc., 1977.

3. Karlekar, B. V. and Desmond, R. M., Engineering Heat Transfer, West Publishing Company, 1977, pp. 75-83.

4. Langmuir, I., Adams, E. Q. and Meikle, G. S., "Flow of Heat Through Furnace Walls: The Shape Factor," American Electrochemical Society, Transactions, Vol. 24, 1913.

5. Harrje, D., et al., "Automated Instrumentation for Building Air Infiltration Measurements," Report No. 13, Center for Environmental Studies, Princeton University, 1975.

6. Harrje, D. and Grot, R., "Instrumentation for Monitoring Energy Usage in Buildings at Twin Rivers," Energy and Buildings, Vol. 1, April 1978.

7. Malik, N., "Field Studies of Dependence of Air Infiltration on Outside Temperature and Wind," Energy and Buildings, Vol. 1, April 1978.

8. Personal discussion with Dr. Jan Beyea.

9. Sinden, F., "Wind, Temperature and Natural Ventilation - Theoretical Considerations," Energy and Buildings, Vol. 1, April 1978.

10. Malinowski, H. K., "Wind Effects on the Air Movement Inside Buildings," Proceedings, Third International Conference on Wind Effects on Buildings and Structures, Tokyo, 1971.

11. Sonderegger, R. C., "Dynamic Models of House Heating Based on Equivalent Thermal Parameters," Report No. 57, Center for Environmental Studies, Princeton University, 1977.

TABLE 1 PROPERTIES OF TEST CHAMBER MATERIALS

Material	ρ (kg/m^3)	c (Wh/kg-°C)	κ (W/m-°C)	d (m)	U (W/m^2-°C)	C_s Wh/m^2-°C)
Plywood	540	0.336	0.115	0.016	7.19	2.9
"	"	"	"	0.009S	12.1	1.7
Studs*	510	0.383	0.118	0.089	1.33	17.4
Fiberglass Insulation	14	0.210	0.047	0.089	0.528	0.3
"	"	"	"	0.152	0.309	0.4
Polystyrene Insulation	16	0.441	0.035	0.025	1.40	0.2
Door	510**	0.383**	0.118**	0.044	2.68	8.6
Masonite	800	0.360	0.106	0.0064	16.6	1.8
Indoor Film Coefficient (Vertical)					8.28	
Indoor Film Coefficient (Horizontal)					9.25	
Outdoor Film Coefficient (4.5m/s wind)					26.2	

* One dimensional heat transfer only
** Estimate
Conductance U = k/d
Capicitance (Capacity per unit area) $C_s = \rho cd$

ρ = Density
c = Specific Heat
k = Conductivity
d = Thickness

TABLE 1 PROPERTIES OF TEST CHAMBER MATERIALS

Material	ρ (kg/m^3)	c (Wh/kg-°C)	κ (W/m-°C)	d (m)	U (W/m^2-°C)	C_s Wh/m^2-°C)
Plywood	540	0.336	0.115	0.016	7.19	2.9
"	"	"	"	0.009S	12.1	1.7
Studs*	510	0.383	0.118	0.089	1.33	17.4
Fiberglass Insulation	14	0.210	0.047	0.089	0.528	0.3
"	"	"	"	0.152	0.309	0.4
Polystyrene Insulation	16	0.441	0.035	0.025	1.40	0.2
Door	510**	0.383**	0.118**	0.044	2.68	8.6
Masonite	800	0.360	0.106	0.0064	16.6	1.8
Indoor Film Coefficient (Vertical)					8.28	
Indoor Film Coefficient (Horizontal)					9.25	
Outdoor Film Coefficient (4.5m/s wind)					26.2	

* One dimensional heat transfer only
** Estimate
Conductance U = k/d
Capicitance (Capacity per unit area) $C_s = \rho cd$

ρ = Density
c = Specific Heat
k = Conductivity
d = Thickness

TABLE 2 DESCRIPTION, OVERALL U-VALUES AND OVERALL THERMAL MASS OF WALLS, ROOF AND FLOOR

Walls	U (W/m^2-°C)	R = 1/U	C_s (Wh/m^2-°C)
Indoor film coefficient	8.28	0.121	0.0
2.5 cm Polystyrene	1.40	0.714	0.2
R-11 Insulation/Studs*	0.605	1.653	1.9
1.6 cm Plywood	7.19	0.139	2.9
Outdoor film coefficient	26.2	0.038	0.0
		R = 2.665	5.0 Wh/m^2-°C
	U = 0.38 W/m^2 °C [R-14.9]		
Roof			
Indoor film coefficient	9.25	0.108	0.0
Plywood**	18.3	0.055	1.1
2.5 cm Polystyrene	1.40	0.714	0.2
R-11 Insulation/Studs*	0.624	1.603	2.4
1.6 cm Plywood	7.19	0.139	2.9
Outdoor film coefficient	26.2	0.038	0.0
		R = 2.657	6.6 Wh/m^2-°C
	U = 0.38 W/m^2 -°C [R-14.9]		
Floor			
Indoor film coefficient	9.25	0.108	0.0
0.6 cm Masonite	16.6	0.060	1.8
2.5 Polystyrene	1.40	0.714	0.2
1.6 cm Plywood	7.19	0.139	2.9
R-11 Insulation/Studs*	0.624	1.603	2.4
0.9 cm Plywood	12.1	0.083	1.7
Outdoor film coefficient	26.2	0.038	0.0
		2.745	9.0 Wh/m^2-°C
	U = 0.36 W/m^2 -°C [R-15.8]		

* Aggregated as described in text

** Estimated as described in text

TABLE 3 FIRST ORDER LOSSINESS

U_{wall}	= 0.38 W/m^2 -°C	A_{wall}	= 7.70 m^2
U_{roof}	= 0.38 W/m^2 -°C	A_{roof}	= 4.69 m^{2*}
U_{floor}	= 0.36 W/m^2 -°C	A_{floor}	= 4.69 m^{2*}

$$\text{Lossiness} = 4\,U_w A_w + U_r A_r + U_f A_f$$

$$= 11.7 + 1.8 + 1.7$$

$$= 15.2 \ W/°C$$

*Does not include area at pipe and its insulation

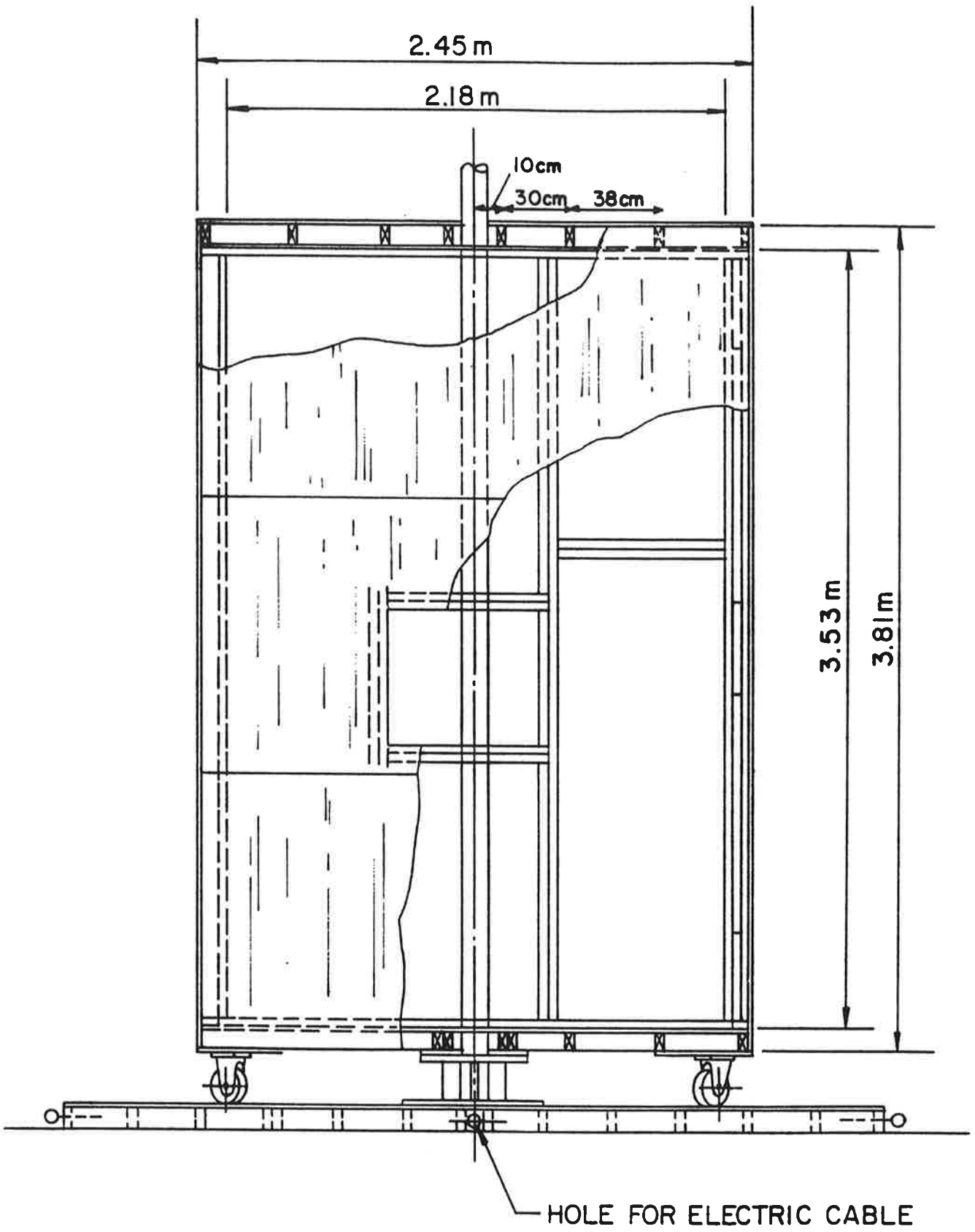

FIGURE 1. SIDE VIEW OF TEST CHAMBER

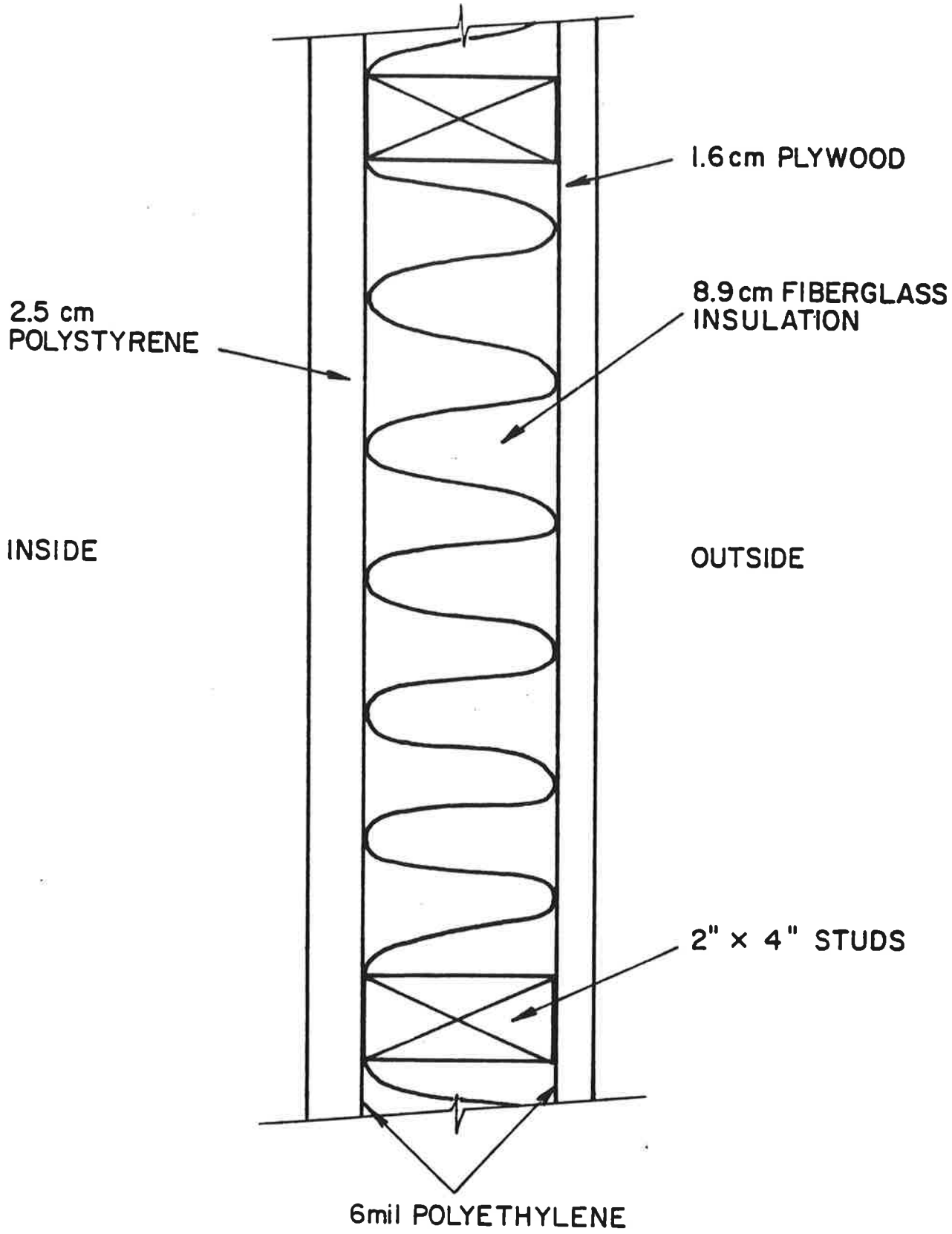

FIGURE 2. TYPICAL WALL SECTION, TOP VIEW

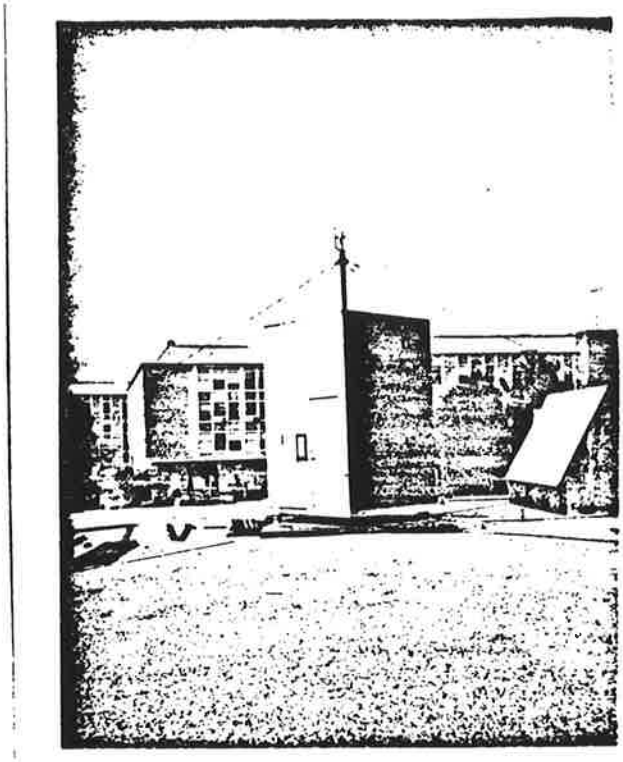

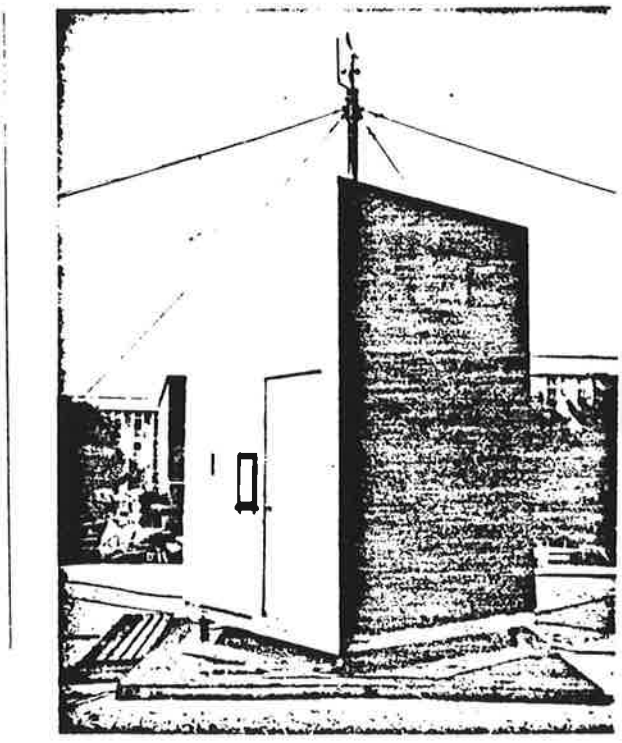

Figure 3. Photographs of Test Chamber

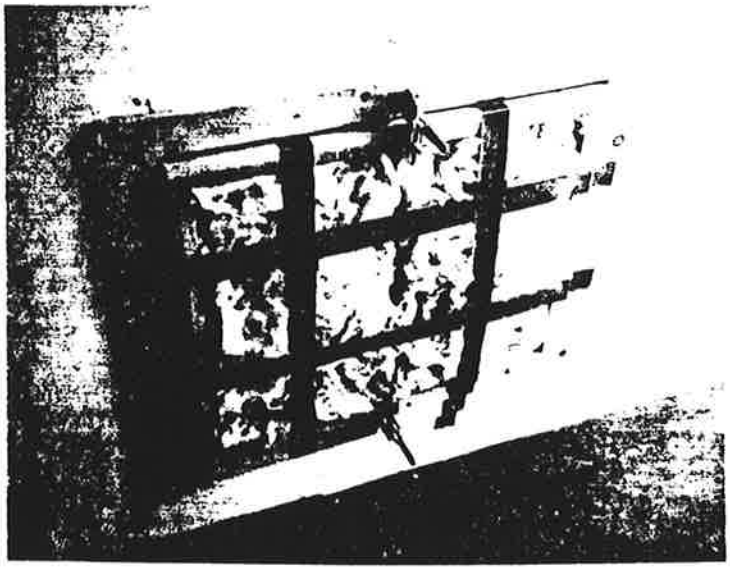

Figure 4. Photograph of Window with
Insulation Panel in Place

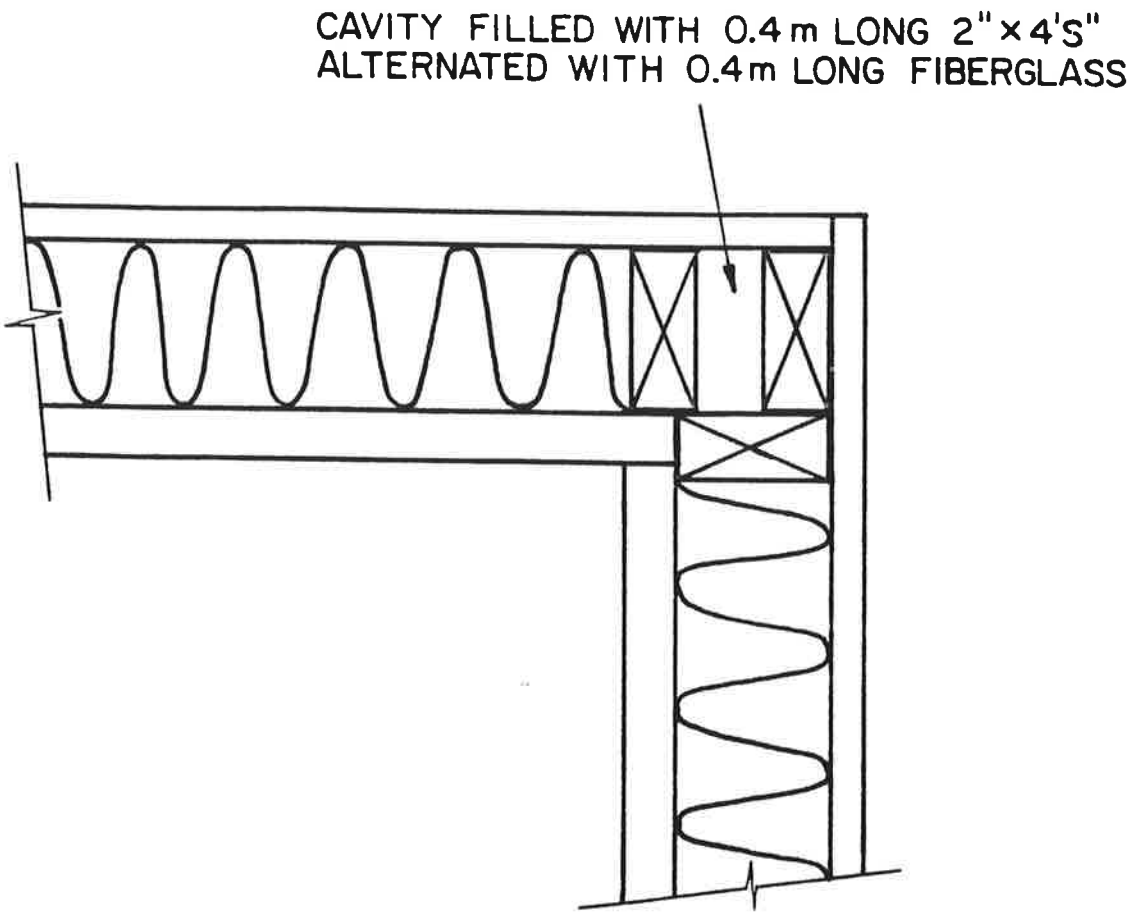

FIGURE 5A. TOP VIEW OF CORNER

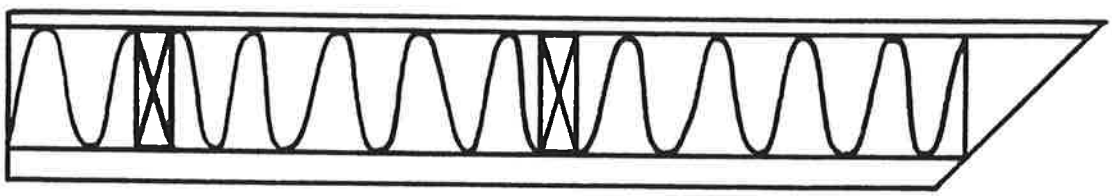

FIGURE 5B. TOP VIEW OF A HALF WALL SECTION

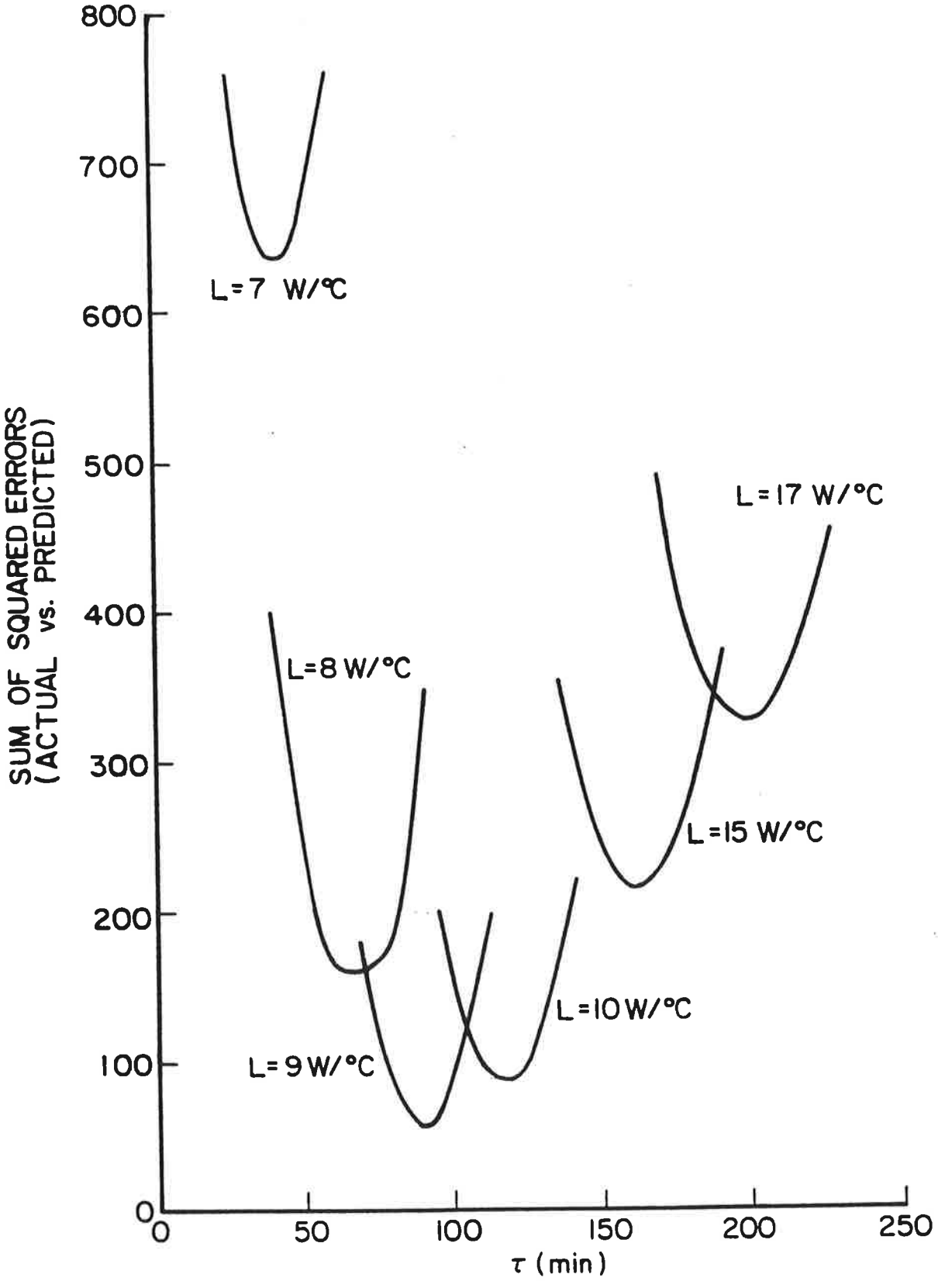

FIGURE 6. TIME CONSTANT vs. FIT OF INTERIOR TEMPERATURE MODEL

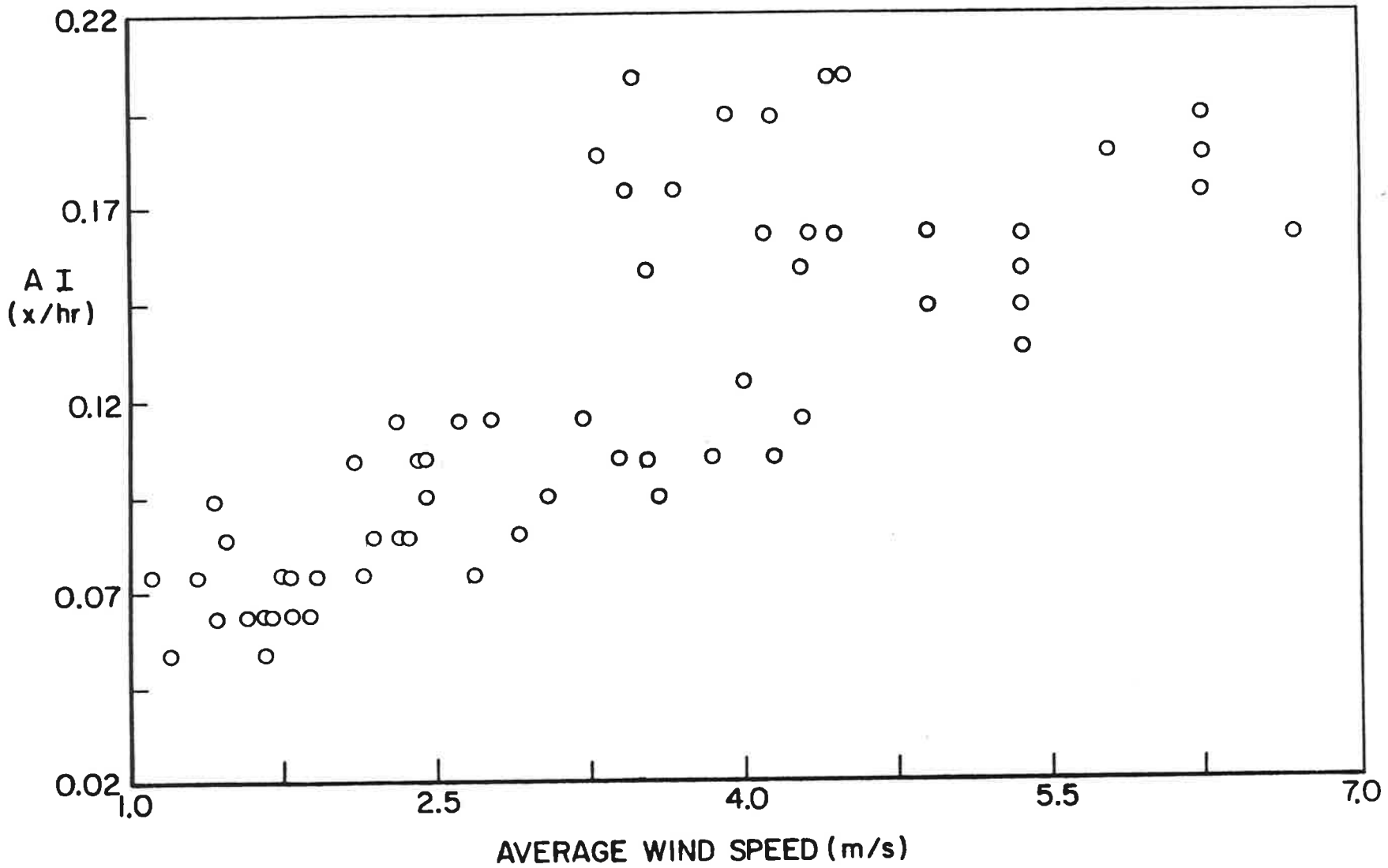

FIGURE 7. AIR INFILTRATION RATE vs. WIND SPEED

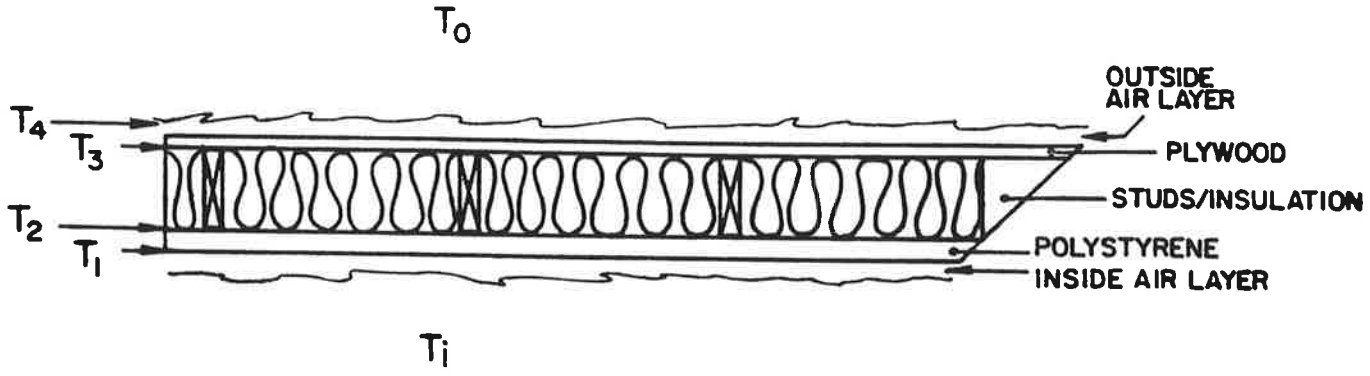

FIGURE A1. WALL SECTION FOR CORNER CALCULATION

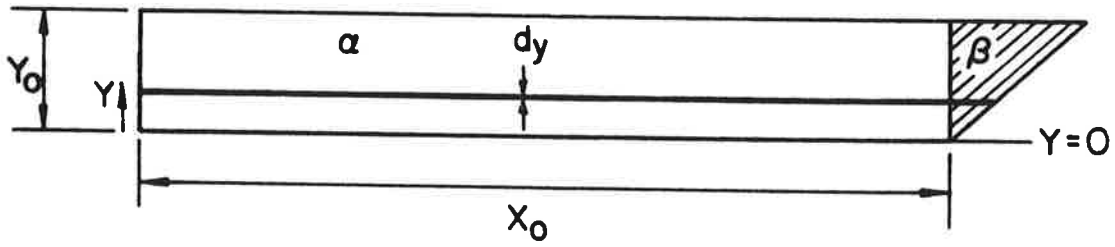

FIGURE A2. STUD/INSULATION LAYER

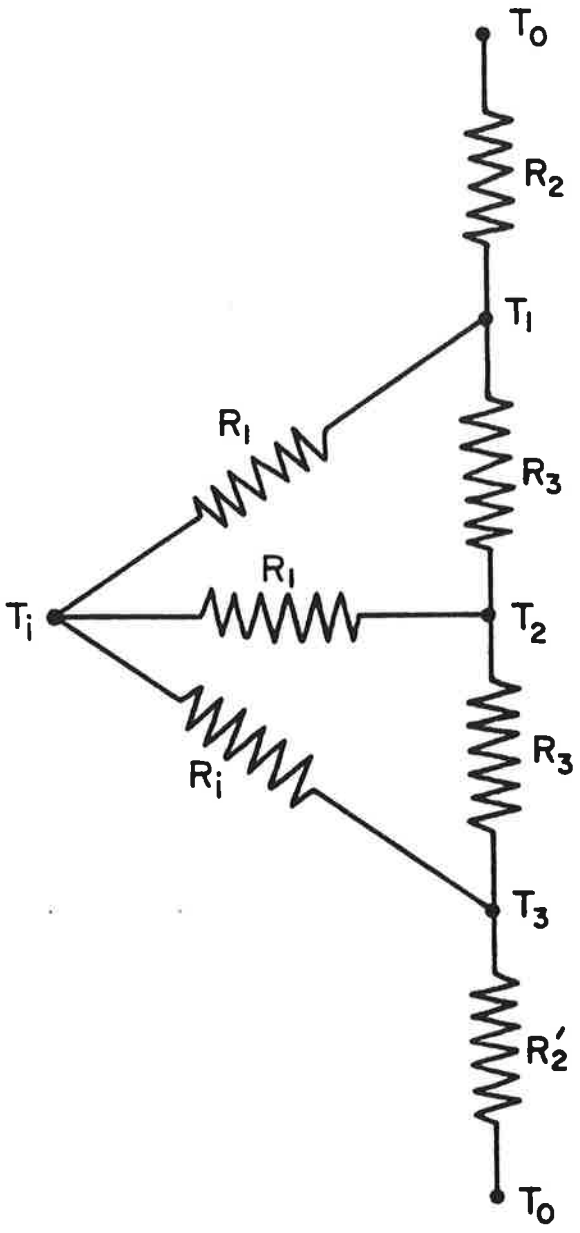

FIGURE B1. RESISTANCE NETWORK OF STEEL MAST